

Weak-Disorder Expansion for the Anderson Model on a Tree

Jeffrey D. Miller¹ and Bernard Derrida^{1,2}

Received December 14, 1993

We show how certain properties of the Anderson model on a tree are related to the solutions of a nonlinear integral equation. Whether the wave function is extended or localized, for example, corresponds to whether or not the equation has a complex solution. We show how the equation can be solved in a weak-disorder expansion. We find that, for small disorder strength λ , there is an energy $E_c(\lambda)$ above which the density of states and the conducting properties vanish to all orders in perturbation theory. We compute perturbatively the position of the line $E_c(\lambda)$ which begins, in the limit of zero disorder, at the band edge of the pure system. Inside the band of the pure system the density of states and conducting properties can be computed perturbatively. This expansion breaks down near $E_c(\lambda)$ because of small denominators. We show how it can be resummed by choosing the appropriate scaling of the energy. For energies greater than $E_c(\lambda)$ we show that nonperturbative effects contribute to the density of states but we have been unable to tell whether they also contribute to the conducting properties.

KEY WORDS: Localization; tree; weak-disorder expansion; mobility edges.

1. INTRODUCTION

Anderson localization,⁽¹⁾ or the study of transport properties of a quantum particle in a random potential, is one of the most important problems in the theory of disordered systems.^(2,3) In one and two dimensions an arbitrarily small random potential suffices to localize all energy eigenstates. In three and higher dimensions both localized and extended states can exist: strong disorder or energies far from the band center give rise to localized states, whereas weak disorder and energies close to the band

¹ Service de Physique Théorique, CE Saclay F-91191 Gif-sur-Yvette Cedex, France.

² Laboratoire de Physique Statistique, Ecole Normale Supérieure, 75231 Paris Cedex 05, France.

center produce extended states. Extended and localized states are separated by a line in the energy–strength of disorder plane, the mobility edge. The location of the mobility edge is a question of fundamental interest.⁽⁴⁾

As usual in statistical mechanics, the simplest cases one can consider are mean-field models. The most extensively studied mean-field model of localization is the Anderson model on a tree.^(5–12) Various approaches have been developed, based in particular on self-energy calculations^(4,5) or on supersymmetry^(8,9,13) which reduce the problem to a nonlinear integral equation.^(5–9) This integral equation, however, is complicated and the position of the mobility edge cannot be determined without recourse to some kind of approximation. Several works tried to overcome this difficulty by considering simplified versions of the model on a tree.^(14,15)

In the present paper, we reconsider the Anderson problem on a tree. We first give a derivation of the integral equation to be solved which is, although completely equivalent to, more intuitive, we think, than previous derivations. The system insulates or conducts depending on whether the integral equation possesses real or complex solutions. We try to solve this equation in the limit of weak disorder using a method⁽¹⁶⁾ which generalizes previous weak-disorder calculations in one dimension.⁽¹⁷⁾

One interesting outcome of this approach is the existence of a line $E_c(\lambda)$ in the E, λ plane (E is the energy and λ measures the strength of disorder) beyond which the integrated density of states and the conducting properties vanish to all orders in perturbation theory. This line tends to the band edge of the pure system, $E = 2\sqrt{K}$ (where $K + 1$ is the coordination number of the tree) in the limit of zero disorder. We can show that for energies greater than $E_c(\lambda)$, nonperturbative contributions to the density of states make it nonzero. We have not, however, been able to determine whether nonperturbative effects also contribute to the conducting properties. The question is of particular interest because Abou-Chacra and Thouless⁽⁶⁾ predict that the mobility edge tends to $E = K + 1$ rather than to the band edge, $E = 2\sqrt{K}$, in the limit of zero disorder.

The paper is organized as follows: In Section 2, we derive the nonlinear integral equation satisfied by the distribution $P(R)$ of a Riccati variable R , defined to be the ratio of the wave function at adjacent sites on the lattice. We show how the solution of this nonlinear integral equation gives the integrated density of states and why the existence of a complex solution is related to the existence of extended states. In Section 3, we discuss the pure system, i.e., the problem in absence of disorder. In Section 4, we show how a weak-disorder expansion can be performed for energies inside the band of the pure system. We find that in the presence of weak disorder the system conducts. In Section 5, we extend the weak-disorder expansion to the neighborhood of the band edge. We obtain within this perturbative

approach an expression for the mobility edge $E_c(\lambda)$ in powers of the strength λ of the disorder. For $E > E_c(\lambda)$, the integrated density of states vanishes to all orders in λ , although it is known that for distributions of the potential with unbounded support, it never vanishes.⁽¹⁸⁻²⁰⁾ In Section 6, we discuss the origin of nonperturbative effects for energies outside the band of the pure system. Lastly, in Section 7, we describe a numerical method to obtain the mobility edge, and we compare the results of this approach with the prediction of Section 5 and with an exactly soluble case where the Riccati variables are independent.

2. FORMULATION OF THE PROBLEM

We consider a tight-binding model on a Cayley tree of N sites (see Fig. 1) with a random potential V_i at each site i of the lattice. The potentials V_i are independent random variables governed by a probability distribution $\rho(V)$ which we choose to have zero mean ($\langle V_i \rangle = 0$). The Schrödinger equation reads

$$\sum_{j=1}^{K+1} \psi_j = E\psi_i - \lambda V_i \psi_i \quad (1)$$

Here ψ_i is the value of the wavefunction at site i , λ is a parameter that controls the strength of the random potential, E is the energy of the particle, and the sum is over the $K+1$ neighbors of the site i . It is useful to rewrite (1) as a recursion relation.⁽¹⁶⁾ Call the central site of the tree i_0

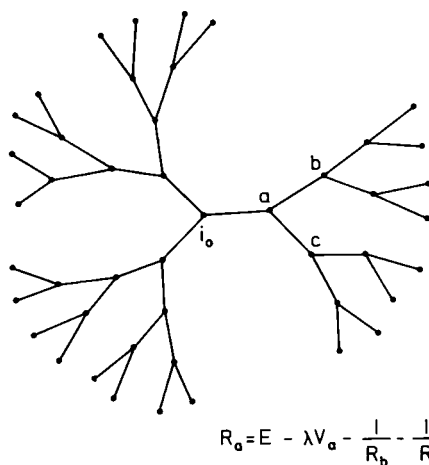


Fig. 1. A Cayley tree with $K=2$ and depth $n=4$.

and define a Ricatti variable R_i on a site i by $R_i = \psi_j / \psi_i$, where j is the neighbor of site i closer to i_0 on the tree. Dividing (1) through by ψ_i and regrouping terms gives (Fig. 1)

$$R_i = E - \lambda V_i - \sum_{j=1}^K \frac{1}{R_j} \quad (2)$$

for all sites except i_0 . This recursion allows one to calculate the R_i associated to all sites of the tree except for the site i_0 (where it is not defined) and except for the sites adjacent to the boundary, where the R_i depend on the boundary conditions and, as we will see later, should be chosen differently depending on the properties we want to study (density of states or conducting properties).

On account of the random potential in (2), the R_i are random variables governed by a probability distribution. The recursion (2) completely determines the probability distribution $P_m(R_i)$ of an R_i located m steps from the boundary of the tree once the probability distribution $P_1(R_i)$ of the R_i on sites adjacent to the boundary have been specified. In what follows we will always choose boundary conditions in such a way that the R_i on sites adjacent to the boundary are identically distributed with distribution $P_1(R)$. The symmetry of the tree then ensures that all the R_i an equal number m of steps from the boundary are also identically distributed with a probability distribution $P_m(R_i)$ that depends on the number m one has to iterate (2). The recursion (2) induces the following recursion on the distributions $P_m(R)$:

$$P_{m+1}(R) = \int \prod_{j=1}^K P_m(R_j) dR_j \int \rho(V) dV \delta \left(R - E + \lambda V + \sum_{j=1}^K \frac{1}{R_j} \right) \quad (3)$$

We shall assume in what follows that, for all the boundary conditions we consider [$P_1(R)$ concentrated on the real axis when we calculate the density of states, or $P_1(R)$ concentrated on the lower half complex plane with all R_i having a negative imaginary part when we study the conduction properties], the recursion (3) converges to a limiting distribution $P(R)$ which satisfies

$$P(R) = \int \prod_{j=1}^K P(R_j) dR_j \int \rho(V) dV \delta \left(R - E + \lambda V + \sum_{j=1}^K \frac{1}{R_j} \right) \quad (4)$$

Up to a change of variables, this integral equation is equivalent to the integral equations obtained in refs. 5-9. A similar equation also exists for diluted lattices.⁽²¹⁻²³⁾ The particular limiting distribution to which (3) converges might depend on the initial $P_1(R)$. We will see below that the

localized and the extended regimes correspond to one of the two following situations:

In the localized region: There is only one fixed distribution, $P_{\text{real}}(R)$, which solves (4). This distribution is concentrated on the real axis and is stable, i.e., it is the limit of the sequence $P_m(R)$ obtained through the recursion (3) for any initial distribution $P_1(R)$ [all initial distributions concentrated on the real axis as well as those concentrated initially in the complex plane converge to this distribution $P_{\text{real}}(R)$, so that even if the R have initially some imaginary part, they become real under the iteration of (2)].

In the extended region: There exist two different fixed distributions, $P_{\text{real}}(R)$ and $P_{\text{complex}}(R)$, which solve (4). The real distribution $P_{\text{real}}(R)$, concentrated on the real axis, is the limit of the sequence $P_m(R)$ when the initial distribution $P_1(R)$ is concentrated on the real axis. This distribution $P_{\text{real}}(R)$ is, however, unstable against imaginary perturbations: a small imaginary component in the R_i on the boundary will not vanish under iteration of (2). Instead, if, as for the scattering situation described below, the initial distribution $P_1(R)$ is concentrated in the lower half complex plane (so that the initial R all have a negative imaginary part), $P_m(R)$ converges to a different distribution $P_{\text{complex}}(R)$ concentrated in the lower half-plane. [Note that there exists also a third distribution in the upper half-plane symmetric to $P_{\text{complex}}(R)$, but we will not consider it because with the boundary conditions we use, all the R_i are always either real or complex with negative imaginary parts.]

The two fixed distributions $P_{\text{real}}(R)$ and $P_{\text{complex}}(R)$ are both solutions of the fixed-point equation (45) and a great deal of what follows is devoted to the study of these fixed distributions.

For choices of E , λ , and $\rho(V)$ such that (4) has both a real and a complex fixed distribution (the extended phase), $P_{\text{real}}(R)$ and $P_{\text{complex}}(R)$ are not independent. In the appendix we show that the real fixed distribution $P_{\text{real}}(R)$ solution of (4) is given in terms of $P_{\text{complex}}(R)$ by

$$\begin{aligned}
 P_{\text{real}}(R) &= \frac{1}{\pi} \int_{-\infty}^{\infty} dr \int_0^{\infty} ds \frac{s}{(R-r)^2 + s^2} P_{\text{complex}}(r-is) \\
 &= \frac{-1}{\pi} \text{Im} \left\{ \int_{-\infty}^{\infty} dr \int_0^{\infty} ds \frac{1}{R-r+is} P_{\text{complex}}(r-is) \right\} \quad (5)
 \end{aligned}$$

We now address the question of the choice of the initial distribution $P_1(R)$ and discuss how the fixed distributions $P_{\text{real}}(R)$ and $P_{\text{complex}}(R)$ are related to the density of states and to the conducting properties.

2.1. The Density of States

Let us first discuss how the density of states can be obtained for the tree geometry⁽¹⁶⁾ (see Fig. 1). We want to calculate the eigenvalues with the boundary condition that the wavefunction vanishes on the boundary of the tree. With this boundary condition, the Schrödinger equation for a site i adjacent to the boundary reads

$$\psi_j = E\psi_i - \lambda V_i \psi_i \quad (6)$$

where j is the only neighbor of site i on the tree. Dividing through by ψ_i then gives

$$R_i = E - \lambda V_i \quad (7)$$

where $R_i = \psi_j/\psi_i$. The initial R are real, so they remain real under iteration of (2) and the invariant measure $P(R)$ is concentrated on the real axis.

As discussed in,⁽¹⁶⁾ Eqs. (2) and (7) solve the Schrödinger equation everywhere on the tree except on the central site i_0 . In terms of the R_i , the Schrödinger equation for the central site i_0 reads

$$E - \lambda V_{i_0} - \sum_{j=1}^{K+1} \frac{1}{R_j} = 0 \quad (8)$$

where the sum runs over the $K+1$ neighbors j of site i_0 . All the R_i are functions of E and the values E_x of the energy which satisfy (8) are the eigenenergies.

Expression (8) contains all the information on the density of states but is not easy to use. If, however, one multiplies (8) by the product of all the R_i in the lattice,⁽¹⁶⁾ it becomes a polynomial in E of degree N , where N is the number of lattice sites and the coefficient of highest degree is 1 [for a tree of depth n , the number of sites is $N = (K^n + K^{n-1} - 2)/(K - 1)$]. Therefore, one can write

$$\prod_{\alpha=1}^N (E - E_x) = \left(E - \lambda V_{i_0} - \sum_{j=1}^{K+1} \frac{1}{R_j} \right) \prod_{i \neq i_0} R_i \quad (9)$$

Both sides of this equation are polynomials in E with real coefficients and real roots. To extract the density of states, one can take the logarithm of this equality, for any complex value of the energy E , with the convention that the branch cut runs along the real axis from $-\infty$ to the largest eigenvalue E_x . When the energy approaches the real axis at a certain value E from above, the imaginary part of the left-hand side is just π times the number of eigenenergies larger than E , whereas the imaginary part of the

right-hand side is equal to π times the number of negative R_i [$+1$ when the term $E - \lambda V_{i_0} - \sum_j (1/R_j)$ is negative]. This is because all the R_i as well as the term $E - \lambda V_{i_0} - \sum_j (1/R_j)$ have positive imaginary parts when the energy E is in the upper complex plane [see (2) and (7)]. Therefore the number $\Omega_n(E)$ of eigenvalues greater than E (the integrated density of states) is given by

$$\Omega_n(E) = \Theta \left(\lambda V_{i_0} + \sum_{j=1}^{K+1} \frac{1}{R_j} - E \right) + \sum_{i \neq i_0} \Theta(-R_i) \quad (10)$$

Since the number of negative R_i is equal to the number of nodes of the wave function, we see that the equality (10) between the integrated density of states and the number of nodes of the wave function, well known in one dimension, remains valid for tree structures, as was already discovered by Dhar and Ramaswamy⁽²⁴⁾ in a similar calculation of the eigenmodes of Eden tree.

For a tree of depth n [with $N = (K^{n+1} + K^n - 2)/(K - 1)$ sites], the average over disorder of $\Omega_n(E)$ is given by

$$\begin{aligned} \langle \Omega_n(E) \rangle &= \rho(V_{i_0}) dV_{i_0} \int_{-\infty}^{\infty} \cdots \int_{-\infty}^{\infty} \prod_{j=1}^{K+1} P_n(R_j) dR_j \Theta \left(\lambda V_{i_0} + \sum_{j=1}^{K+1} \frac{1}{R_j} - E \right) \\ &+ (K+1) \sum_{m=1}^n K^{n-m} \int_{-\infty}^0 P_m(R) dR \end{aligned} \quad (11)$$

The expression can be simplified by using the recursion (3),

$$\begin{aligned} \langle \Omega_n(E) \rangle &= \int_{-\infty}^{\infty} P_n(R) dR \int_{-\infty}^{\infty} P_{n+1}(R') dR' \Theta \left(\frac{1}{R} - R' \right) \\ &+ (K+1) \sum_{m=1}^n K^{n-m} \int_{-\infty}^0 P_m(R) dR \end{aligned} \quad (12)$$

The tree geometry has the pathology that the number of sites near the boundary is proportional to the total number of sites in the tree. Surface effects are therefore strong. One can see this in (12), where $P_1(R)$ is multiplied by the largest power of K . To eliminate these boundary effects and obtain an expression for the behavior of the bulk, one can use a subtraction procedure. Letting F_n be an extensive quantity in a tree of depth n , the quantity $(F_n - KF_{n-1})/2$ is the value of F per site far from the boundary when n is large.⁽¹⁶⁾ To see this, note that the number of sites m steps from the boundary in a tree of depth n equals K times the number of sites m steps from the boundary in a tree of depth $n-1$. The contributions to

F from sites m steps from the boundary are thus canceled in the subtraction. Under this subtraction, the number of sites we are left with is

$$(K^{n+1} + K^n - 2)/(K - 1) - K(K^n + K^{n-1} - 2)/(K - 1) = 2$$

sites which are far from the boundary. Thus, dividing the difference $F_n - KF_{n-1}$ by two gives the value of F per site far from the boundary. Applying this subtraction to (12) gives the average integrated density of states $\langle \omega(E) \rangle$ per site far from the boundary in the limit $n \rightarrow \infty$,

$$\begin{aligned} \langle \omega(E) \rangle = & -\frac{K-1}{2} \int_{-\infty}^{\infty} P_{\text{real}}(R) dR \int_{-\infty}^{\infty} P_{\text{real}}(R') dR' \Theta\left(\frac{1}{R} - R'\right) \\ & + \frac{K+1}{2} \int_{-\infty}^0 P_{\text{real}}(R) dR \end{aligned} \quad (13)$$

For values of E and λ such that there exists a complex fixed distribution $P_{\text{complex}}(R)$, one can use the relation (5) between P_{real} and P_{complex} to express $\langle \omega(E) \rangle$ in terms of this complex distribution (see the appendix),

$$\begin{aligned} \langle \omega(E) \rangle = & \frac{1}{\pi} \text{Im} \left\{ \frac{K-1}{2} \int P_{\text{complex}}(R) dR \int P_{\text{complex}}(R') dR' \log\left(R' - \frac{1}{R}\right) \right. \\ & \left. - \frac{K+1}{2} \int P_{\text{complex}}(R) dR \log(R) \right\} \end{aligned} \quad (14)$$

2.2. The Conducting Properties

We turn now to the relation between $P(R)$ and the conducting properties of the system. Imagine the situation shown in Fig. 2. Attach a wire to each boundary site of a branch of a tree as shown in Fig. 2. Suppose then that one sends a plane wave in at the left and allows it to scatter off the tree. For a branch of finite depth, some of the incoming wave will be reflected and some will propagate through the branch to the wires on the right. Of interest is what happens when the depth of the branch becomes large. There are two possibilities: either the wave is entirely reflected or some of the wave propagates through the tree into the wires on the right. In the former case, either there is a gap in the energy spectrum or the wavefunctions of the tree are localized; in the latter case the wavefunctions are extended. Now it is known that for a potential with unbounded support (e.g., a Gaussian)⁽¹⁸⁻²⁰⁾ there are states at all energies. In this case, a reflection amplitude of modulus 1 (complete reflection of the wave) implies that the states at that energy are localized. Therefore, to determine whether at

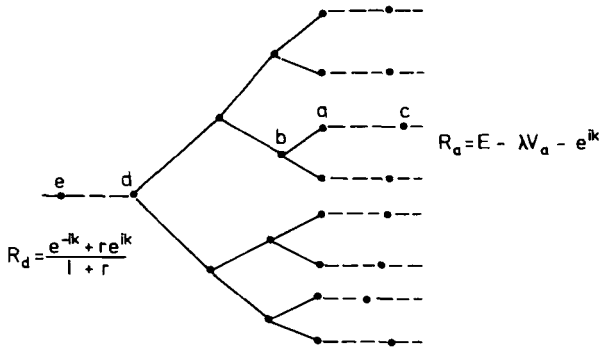


Fig. 2. A branch of a Cayley tree with wires attached to the boundaries to test the conducting properties. In the scattering situation, a plane wave is sent in from the left and allowed to scatter off the tree.

a given value of E and λ the particle is localized, it suffices to compute the reflection amplitude in this experiment.

To relate the reflection amplitude to the Ricatti variables, one needs to analyze what happens at the boundary. First consider the Schrödinger equation for a site a adjacent to the right boundary,

$$\psi_b + \psi_c = E\psi_a - \lambda V_a \psi_a \tag{15}$$

where b and c are the neighbors of a on the tree and in the wire, respectively (Fig. 2). In the wire the wavefunction is a plane wave $\psi = e^{ikx}$ going to the right (corresponding to no incoming flux from right infinity) so that $\psi_c/\psi_a = e^{ik}$. The Ricatti variable $R_a = \psi_b/\psi_a$ thus equals

$$R_a = E - \lambda V_a - e^{ik} \tag{16}$$

The wave vector k can be adjusted by putting a uniform potential on the wire. We note that the R_a for all sites adjacent to the boundary have a negative imaginary part and it is easy to check that the iteration (2) preserves this property.

Starting with the boundary R_a given by (16), we now iterate the recursion (2) up to the first R in the wire on the left side of the tree (Fig. 2). At this boundary we have both an incoming and an outgoing wave, so that the wave function on the left wire has the form $\psi = e^{ikx} + r e^{-ikx}$, where r is the reflection amplitude. The reflection amplitude r is therefore related to the Ricatti variable R_d by

$$R_d = \frac{\psi_e}{\psi_d} = \frac{e^{-ik} + r e^{ik}}{1 + r} \tag{17}$$

or equivalently,

$$r = -\frac{R_d - e^{-ik}}{R_d - e^{ik}} \quad (18)$$

It is clear that if R_d is real, the numerator and the denominator are complex conjugates and so $|r| = 1$. It is also easy to see that if R_d has a negative imaginary part, $|r| < 1$. Thus if the imaginary parts of the initial R_i iterate to zero, the particle is totally reflected and if they do not, the particle has a nonzero transmission coefficient. To find the mobility edge it therefore suffices to study the complex fixed distribution $P_{\text{complex}}(R)$ and to determine at which values of E and λ the probability of finding a nonzero imaginary part of R first vanishes.

Remark. An idealized scattering situation like the one shown in Fig. 2 can be used in other cases, including finite-dimensional lattices, to decide whether a system is conducting or insulating. One could have, for example, an incoming wave on a wire attached to an internal site and outgoing waves at the boundary. A straightforward calculation but which would require new notations (that we will not present here) would show that a reflection amplitude smaller than 1 in the scattering situation is equivalent to the Green's function having a nonvanishing imaginary part when the energy E tends to the real axis (refs. 25 and 26 and references therein).

For arbitrary λ , E , and $\rho(V)$, one does not know how to find the fixed distributions that solve (4) and in the following sections we will show how certain quantities can be expanded in the limit of weak disorder (λ small). An exception is when the distribution of the potential is Cauchy⁽⁵⁾

$$\rho(V) = \frac{1}{\pi} \frac{1}{V^2 + 1} \quad (19)$$

Using the fact that sums of Cauchy random variables are also Cauchy distributed and that the inverse of a Cauchy variable is Cauchy, it is easy to obtain the exact form of $P_{\text{real}}(R)$:

$$P_{\text{real}}(R) = \frac{1}{\pi} \frac{b}{(R-a)^2 + b^2} \quad (20)$$

where the parameters a and b are the values of the attractive fixed point of the following two-dimensional map:

$$a_{n+1} = E - K \frac{a_n}{a_n^2 + b_n^2}; \quad b_{n+1} = \lambda + K \frac{b_n}{a_n^2 + b_n^2}$$

Using (13), one then finds the following closed expression for the integrated density of states $\langle \omega(E) \rangle$:

$$\langle \omega(E) \rangle = \frac{K+1}{2\pi} \tan^{-1} \left(\frac{b}{a} \right) - \frac{K-1}{2\pi} \tan^{-1} \left(\frac{b}{a} \frac{a^2 + b^2 + 1}{a^2 + b^2 - 1} \right) \quad (21)$$

Unfortunately, no one has been able to obtain an exact expression for the complex fixed distribution, even in the case of a Cauchy-distributed potential. So conduction properties such as the location of the mobility edge are not known exactly even for Cauchy disorder.

3. THE PURE SYSTEM

Before proceeding to the weak-disorder expansions, let us consider the case of no disorder ($\lambda = 0$). For zero disorder and for our choices of boundary conditions, all the R_i for the boundary sites are equal, and so the initial distribution $P_1(R)$ is a δ -function. In the absence of disorder, all the $P_k(R)$ computed from $P_1(R)$ through the recursion (3) are also δ -functions concentrated at some value A_k ,

$$P_k(R) = \delta(R - A_k) \quad (22)$$

where the A_k satisfy the following recursion:

$$A_{k+1} = E - \frac{K}{A_k} \quad (23)$$

This recursion for A_k has two fixed points which are real when $|E| > 2\sqrt{K}$ and complex conjugate when $-2\sqrt{K} < E < 2\sqrt{K}$.

First, if

$$E > 2\sqrt{K} \quad (24)$$

the sequence A_k given by the recursion (23) always converges to the real fixed point A given by

$$A = \frac{E + (E^2 - 4K)^{1/2}}{2} \quad (25)$$

This implies that in the scattering situation described in Section 2, the initial complex R_i becomes real under iteration, and hence the wave is completely reflected. Furthermore, the integrated density of states is zero for this range of energy. To see this, note that with the boundary condition (7) (i.e., $R_i = E$), appropriate for the calculation of the density of states,

$A_1 > A_2 > \dots > A_n \dots > A$, and so all the R are positive. Moreover, $E - (K+1)/A_n$ is also positive. It then follows from expression (10) or (13) that the integrated density of states is zero for the range of energy (24), meaning that even for a finite tree, there is no eigenenergy greater than $2\sqrt{K}$ and so the range of energy (24) is outside the band. The case $E < -2\sqrt{K}$ is obviously symmetric.

On the other hand, if

$$-2\sqrt{K} < E < 2\sqrt{K} \quad (26)$$

there exists a complex fixed point of (23),

$$A = \frac{E - i(4K - E^2)^{1/2}}{2} \quad (27)$$

meaning that there is a δ -distribution concentrated at this point that solves (3).

If one starts with a real A_1 as in (7) to compute the density of states, the sequence A_k does not converge. Letting the energy $E = 2\sqrt{K} \cos \theta$, one finds

$$A_n = \sqrt{K} \frac{\sin(n\theta + \theta)}{\sin(n\theta)} \quad (28)$$

The integrated density of states for a tree of depth n then follows from (11):

$$\begin{aligned} \Omega_n(E) = & \Theta \left(\frac{\sin n\theta - K \sin(n\theta + 2\theta)}{\sin(n\theta + \theta)} \right) \\ & + (K+1) \sum_{m=1}^n K^{n-m} \Theta \left(\frac{-\sin(m\theta + \theta)}{\sin(m\theta)} \right) \end{aligned} \quad (29)$$

The spectrum consists of a finite number of eigenvalues (as it should for a finite system) with huge degeneracies which reflect the symmetries of the tree.

If one starts with a complex A_1 , the sequence (23) does not converge either. It is, however, easy to show that

$$\frac{A_k - \sqrt{K} e^{i\theta}}{A_k - \sqrt{K} e^{-i\theta}} = e^{-2(k-1)i\theta} \frac{A_1 - \sqrt{K} e^{i\theta}}{A_1 - \sqrt{K} e^{-i\theta}} \quad (30)$$

From this explicit expression, we see that if A_1 is complex, A_k remains complex, and so the system is conducting.

Remark. It is a property particular to the pure system that when the R_i at the boundary are all equal, the sequence A_n does not converge, and thus the sequence $P_k(R)$ has no limit. As soon as one introduces disorder ($\lambda \neq 0$), there are limiting distributions $P_{\text{real}}(R)$ and $P_{\text{complex}}(R)$ which satisfy the fixed point (4). These distributions, in the limit $\lambda \rightarrow 0$, also satisfy the fixed-point equation (4). It is possible to find these limiting distributions. The complex distribution is a δ -function concentrated at A given by (27) and the real distribution is given by the relation (5) between $P_{\text{real}}(R)$ and $P_{\text{complex}}(R)$,

$$P_{\text{real}}(R) = \frac{1}{2\pi} \frac{(4K - E^2)^{1/2}}{R^2 - ER + K} \quad (31)$$

It is interesting to notice that this fixed distribution (31) is the invariant measure of the map (23). Using this fixed distribution, one obtains the following expression for the integrated density of states $\omega(E)$ per site far from the boundary:

$$\omega(E) = \frac{K+1}{2\pi} \theta - \frac{K-1}{2\pi} \tan^{-1} \left(\frac{K+1}{K-1} \tan \theta \right) \quad (32)$$

4. WEAK-DISORDER EXPANSION INSIDE THE BAND

We turn now to the weak-disorder expansions. As the properties of the pure system are qualitatively different in the band and outside the band, the weak-disorder expansion requires rather different techniques in these two cases. We will see that the neighborhood of the band edge must also be treated separately.

In this section, we explain the small- λ expansion for energies E inside the band of the pure system ($-2\sqrt{K} < E < 2\sqrt{K}$). In this energy range, we saw that the complex fixed distribution solution of (3) is a δ -function concentrated at the complex number A ,

$$A = \frac{E - i(4K - E^2)^{1/2}}{2} \quad (33)$$

To obtain the weak-disorder expansion we assume that for λ small, the variables R which appear in the recursion (2) have small fluctuations around A (see Fig. 3 and Remark 1 at the end of this section), so that the distribution $P_{\text{complex}}(R)$ remains concentrated around A . In accordance

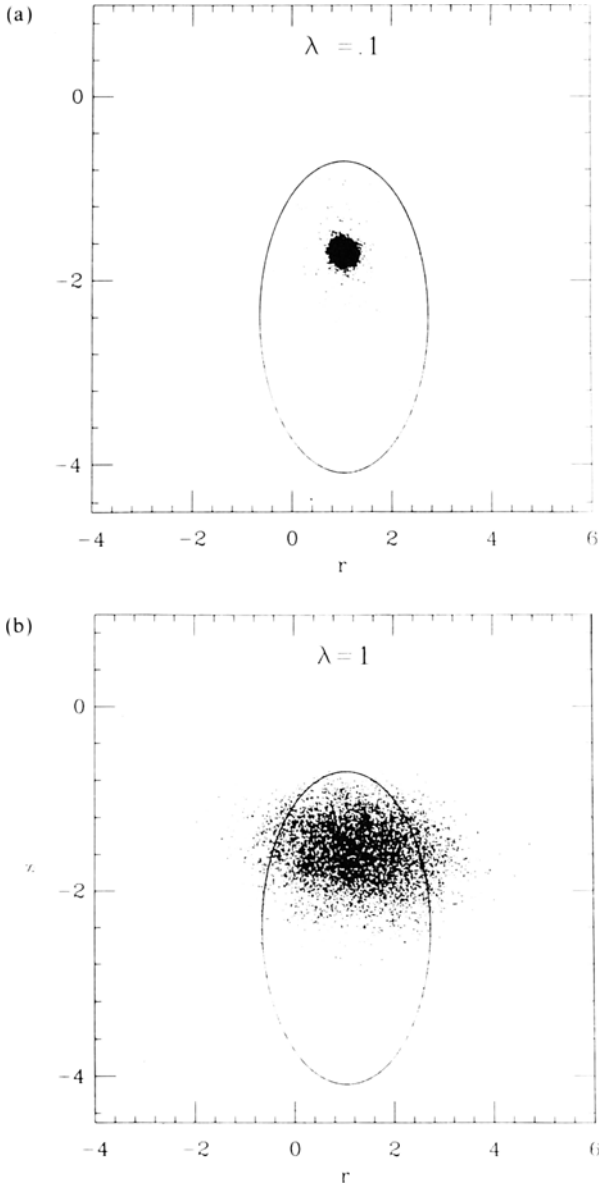


Fig. 3. A set of typical R obtained by the Monte Carlo version of the recursion (2) explained in Section 7 for $N=1000$. Here $K=4$, $E=2.1$, and the complex fixed-point solution of (27), represented by a diamond, lies at $A=1.05-1.702i$. The ellipse represents the set of points to which the initial $R=2-i$ would map in the absence of disorder. For small disorder, (a) $\lambda=0.1$, the R quickly move off the ellipse and concentrate themselves around the complex fixed point. As the disorder increases, (b) $\lambda=1$ and (c) $\lambda=5$, the R spread out. Finally, for very large disorder, (d) $\lambda=30$, the R quickly become real, and the particle is localized.

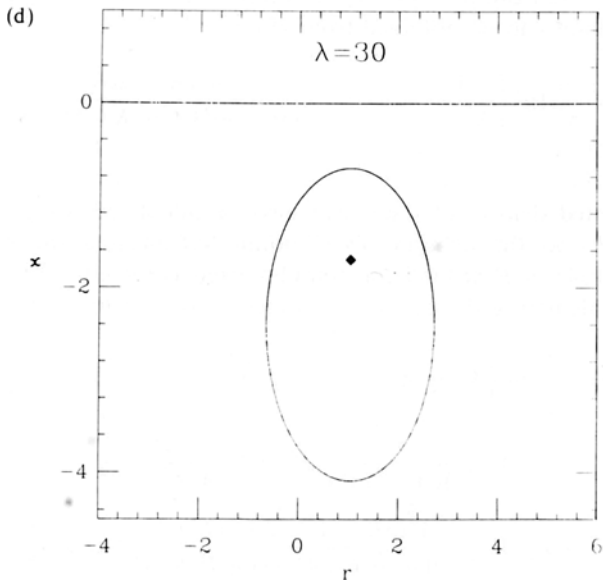
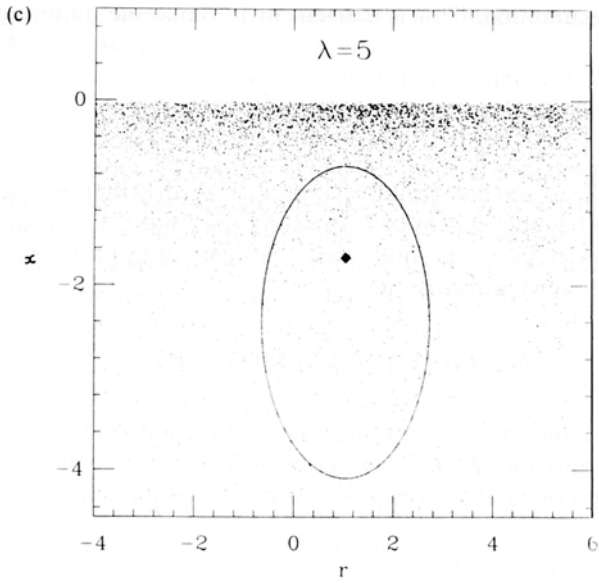


FIGURE 3 (continued)

with this assumption,⁽¹⁶⁾ it is convenient to make the following change of variables:

$$R_i = \frac{A}{1 + \lambda B_i + \lambda^2 C_i + \dots} \quad (34)$$

Here B_i, C_i, \dots are fluctuating quantities, the distributions of which are assumed to be independent of λ . Inserting (34) into (2) and equating terms order by order in λ , one finds that the fluctuating parts B_i, C_i, \dots , of R_i satisfy the following recursions:

$$AB_i = V + \frac{1}{A} \sum_{j=1}^K B_j; \quad AC_i - AB_i^2 = \frac{1}{A} \sum_{j=1}^K C_j \quad (35)$$

and so on. Using these equations, it is easy to compute the moments of the fluctuating variables B_i, C_i, \dots in terms of K, E , and the moments $\langle V^p \rangle$ of the random potential V , which we assume to be finite. For example,

$$\langle B \rangle = 0; \quad \langle B^2 \rangle = \frac{A^2 \langle V^2 \rangle}{A^4 - K}; \quad \langle C \rangle = \frac{A^4 \langle V^2 \rangle}{(A^4 - K)(A^2 - K)} \quad (36)$$

Using this weak-disorder expansion, one can then calculate perturbatively any quantity that can be expressed as a function of the R_i . For example the real fixed point can be obtained from (5),

$$P_{\text{real}}(R) = \frac{-1}{\pi} \text{Im} \left\{ \frac{1}{R - A} + \lambda^2 \langle V^2 \rangle \frac{A^3(A^3 - KR)}{(R - A)^3(A^2 - K)(A^4 - K)} + O(\lambda^3) \right\} \quad (37)$$

The integrated density of states can also be calculated using (14), which relates $\omega(E)$ to the complex fixed point. Substituting the perturbative expansion (34) of R around the complex fixed point into (14), expanding in λ , and calculating the necessary moments, we find to order λ^4

$$\begin{aligned} \omega(E) = & \frac{-1}{\pi} \text{Im} \left\{ K \log A - \frac{K-1}{2} \log(A^2 - 1) - \lambda^2 \langle V^2 \rangle \frac{A^2}{2(A^2 - 1)^2} \right. \\ & - \lambda^3 \langle V^3 \rangle \frac{A^3}{3(A^2 - 1)^3} - \lambda^4 \langle V^4 \rangle \frac{A^4}{4(A^2 - 1)^4} \\ & \left. + \lambda^4 \langle V^2 \rangle^2 \frac{A^4(3K - A^2 - 2A^4)(K + 1)}{4(A^2 - K)(A^4 - K)(A^2 - 1)^4} + O(\lambda^5) \right\} \quad (38) \end{aligned}$$

Higher-order terms in λ are straightforward to calculate but in practice the

algebra required to work out the necessary moments and correlations becomes rather involved.

Conduction properties can be calculated in a similar way. A question of basic interest is whether the wave function is localized or extended. From the discussion of Section 2 we know that the wavefunction is extended if there exists a complex fixed distribution concentrated in the lower half-plane. One way of determining whether such a complex fixed distribution exists is to calculate the magnitude of the reflection amplitude and see whether it is less than (extended) or equal to (localized) 1. The existence of the complex fixed distribution can be determined more easily, however, by considering $\langle \text{Im } R \rangle$. Since the complex fixed distribution is concentrated in the lower half-plane, a necessary and sufficient condition for it to exist is for $\langle \text{Im } R \rangle$ to be nonzero. Perturbatively we have

$$\begin{aligned} \langle \text{Im } R \rangle &= \langle \text{Im} \{ A(1 - \lambda B - \lambda^2 C + \lambda^2 B^2 \dots) \} \rangle \\ &= \text{Im} \left\{ A - \lambda^2 \langle V^2 \rangle \frac{KA^3}{(A^2 - K)(A^4 - K)} \right. \\ &\quad \left. + \lambda^3 \langle V^3 \rangle \frac{KA^4(A^4 + K)}{(A^2 - K)(A^4 - K)(A^6 - K)} + O(\lambda^4) \right\} \end{aligned} \quad (39)$$

Remark 1. Equation (39) indicates that for energies E inside the band of the pure system, weak disorder leaves the eigenfunctions extended. This result, obtained for arbitrary K including $K = 1$, where the tree becomes one-dimensional, apparently contradicts the well-known fact that weak disorder localizes all the eigenfunctions in one dimension.⁽²⁷⁾ The reason the above calculation does not apply when $K = 1$ is that the assumption that the iteration (3) converges for weak disorder to a fixed complex distribution close to the fixed point A is not valid. This can be easily seen in the weak-disorder expansion. Assume that some R_i obtained after n iterations has the form $R_i = A/(1 + \lambda B_i^{(n)} + \dots)$. Clearly one has

$$B_i^{(n)} = \frac{V_i}{A} + \frac{1}{A^2} \sum_{j=1}^K B_j^{(n-1)} \quad (40)$$

This implies the following recursion for $\langle |B^{(n)}|^2 \rangle$:

$$\langle |B^{(n)}|^2 \rangle = \frac{\langle V^2 \rangle}{K} + \frac{\langle |B^{(n-1)}|^2 \rangle}{K} \quad (41)$$

where we have used the equality $|A| = \sqrt{K}$. We see from (41) that for $K > 1$ the fluctuations $\langle |B^{(n)}|^2 \rangle$ saturate as n increases, meaning that an initial distribution concentrated in the neighborhood of A remains concentrated

near A . On the other hand, for $K=1$, the fluctuations grow linearly with n so that the recursion does not converge to a fixed distribution close to A .

Remark 2. The case $K=1$ (one dimension) is special in other respects. In the band, at energy $E=2\sqrt{K}\cos\theta$, the fixed point A is $A=\sqrt{K}e^{-i\theta}$. Hence for $K=1$, there are a large number of values of θ at which the weak-disorder expansion (38) contains small denominators.^(17,28-31) This is not the case for $K>1$, where only the band edges ($\theta=0$ and $\theta=\pi$) seem to give rise to small denominators.

5. NEAR THE BAND EDGE

As E approaches the band edge of the pure system $2\sqrt{K}$ from below at fixed λ , terms like $(A^2-K)^{-1}$ diverge, and the above perturbation theory breaks down. Perturbative information about the complex fixed point can, however, still be obtained by choosing the appropriate scaling of the energy with λ . Let

$$E = \sqrt{K}(2 - a\lambda^2) \quad (42)$$

where a is of order one. For these energies, A is given by $\sqrt{K}[1 - i\lambda\sqrt{a} + O(\lambda^2)]$. Substituting this in the expansions (38) and (39), one finds

$$\langle \omega(E) \rangle = \lambda^3 \frac{2K(K+1)}{3\pi(K-1)^2} \left(a^{3/2} + \frac{3\langle V^2 \rangle a^{1/2}}{2(K-1)} + \frac{3\langle V^2 \rangle^2}{8(K-1)^2 a^{1/2}} + \dots \right) \quad (43)$$

and

$$\langle \text{Im } R \rangle = -\lambda \sqrt{K} \left(a^{1/2} + \frac{\langle V^2 \rangle}{2(K-1) a^{1/2}} + \dots \right) \quad (44)$$

From this we see that the leading term in a small- λ expansion with a fixed as $\lambda \rightarrow 0$ corresponds to resumming an infinite series in the original expansions (38) and (39).

For the range of energies (42), let us make the following change of variable:

$$R_i = \frac{\sqrt{K}}{1 - \phi_i} \quad (45)$$

Substituting this expression in (2), we see that the ϕ_i are of order λ . Expanding both sides of (2) yields

$$\phi_i + \phi_i^2 + \phi_i^3 + \dots = -\frac{\lambda V}{\sqrt{K}} - a\lambda^2 + \frac{1}{K} \sum_{j=1}^K \phi_j \quad (46)$$

The moments of ϕ can then be calculated by taking successive integer powers of this equation. To lowest order one obtains

$$\langle \phi^2 \rangle = -a\lambda^2; \quad \langle \phi \rangle^2 = -\lambda^2 \left(a + \frac{\langle V^2 \rangle}{K-1} \right); \quad \langle \phi \rangle^3 = O(\lambda^3) \quad (47)$$

and so forth. Just as in the last section, we can now calculate the average of functions with respect to the complex fixed point perturbatively. For example, one finds, using (14) for the integrated density of states,

$$\langle \omega(E) \rangle = \lambda^3 \frac{2K(K+1)}{3\pi(K-1)^2} \left(a + \frac{\langle V^2 \rangle}{K-1} \right)^{3/2} + O(\lambda^4) \quad \text{for } a > -\frac{\langle V^2 \rangle}{K-1} \quad (48)$$

and $\langle \omega(E) \rangle = 0$ to order λ^3 for $a < -\langle V^2 \rangle / (K-1)$. Both (47) and (48) agree with (38) and (39) when a becomes large, as it should, and (47) and (48) are expected to represent the resummed series of the most singular terms in the expansions (38) and (39).

One might wonder how this result is modified by higher-order terms. If one decides to calculate the integrated density of states or any other quantity to a given order p in λ , one needs to calculate the first p moments ϕ to order λ^p . To do so, one takes the successive powers of (46) and one averages. This gives relationships between the first p moments of ϕ . If one uses these relations to express all the moments in terms of the first moment $\langle \phi \rangle$, one ends up with a polynomial equation in ϕ of degree p which has real coefficients depending on λ , a , and the moments of the potential V . As one varies a (i.e., the energy E), one finds that two complex roots of this polynomial become real at a certain critical value E_c which to fourth order in λ reads

$$\begin{aligned} \frac{E_c}{\sqrt{K}} = & 2 + \lambda^2 \frac{\langle V^2 \rangle}{K-1} + \lambda^3 \frac{\sqrt{K} \langle V^3 \rangle}{(K-1)} + \lambda^4 \frac{K \langle V^4 \rangle}{(K-1)^3} \\ & - \lambda^4 \frac{(9K^2 - 14K - 3) \langle V^2 \rangle^2}{4(K-1)^4} + O(\lambda^5) \end{aligned} \quad (49)$$

If one pushes this expansion to higher order in λ , one would find higher-order corrections to E_c , but for $E > E_c$, $\langle \phi \rangle$ as well as the higher moments of ϕ would be real, and this implies through (14) that $\omega(E) = 0$ for $E > E_c$ to any order in λ .

This result seems to contradict the well-known fact that the density of states never vanishes for distributions of the random potential with unbounded support (such as the Gaussian distribution).⁽¹⁸⁻²⁰⁾ Our result can be reconciled with a nonzero density of states at all energies E only if

there are small nonperturbative contributions to the density of states above E_c which vanish to any order in λ . We discuss this point in the next section.

If perturbation theory could be trusted, it would follow from the discussion of Section 2 that the particle is localized for energies above E_c since $\langle \phi \rangle$ is real. The perturbative calculation therefore predicts a mobility edge at E_c given by (49). This result could be modified by nonperturbative effects; unfortunately, unlike the case for the density of states, we have not been able to discover what these effects might be or how to calculate them.

6. BEYOND THE BAND EDGE

In this section we consider energies larger than $2\sqrt{K}$ and outside the scaling regime discussed in the last section. In this range of energy, the R_i converge to the real fixed point A given by (25) when $\lambda=0$. For small λ , one expects the R_i to fluctuate about A . Expression (13) for the density of states requires, however, the knowledge of $P_{\text{real}}(R)$ for values of R far from A . This is a large-deviation problem since untypical values of R are produced by untypical values of the potential. We are going to show that the real fixed distribution $P_{\text{real}}(R)$ can be calculated by a saddle point method. We have also tried to calculate the complex fixed distribution in this range of energies by a similar approach but failed and we are unable to tell whether the fixed complex distribution simply does not exist or whether we have just not been able to find it.

Since the regions of R which contribute to the density of states correspond to untypical values of R , the shape of $P_{\text{real}}(R)$ in these regions depends strongly on the shape of $\rho(V)$. In what follows, we will take $\rho(V)$ to be Gaussian,

$$\rho(V) = \frac{1}{(2\pi)^{1/2}} \exp\left(-\frac{V^2}{2}\right) \quad (50)$$

The equation to be solved for $P_{\text{real}}(R)$ is then

$$P(R) = \int \frac{dV}{(2\pi)^{1/2}} \exp\left(-\frac{V^2}{2}\right) \prod_{i=1}^K dR_i P(R_i) \delta\left(R - E + \lambda V + \sum_{i=1}^K \frac{1}{R_i}\right) \quad (51)$$

Now suppose that λ is small and that R has fluctuations of order λ around A . If we write $R = A + \lambda\phi$, we get from (2)

$$\phi = -\lambda V + \frac{1}{A^2} \sum_i \phi_i \quad (52)$$

Since V is Gaussian distributed, it follows that ϕ is also Gaussian with zero mean and $\langle \phi^2 \rangle = \langle V^2 \rangle / (1 - K/A^4)$. In terms of the variable R ,

$$P(R) \simeq \frac{1}{(2\pi\lambda^2\langle\phi^2\rangle)^{1/2}} \exp -\frac{(R-A)^2}{2\lambda^2\langle\phi^2\rangle} \quad (53)$$

valid for $R-A$ of order λ . Given this expression for $P(R)$ valid for small fluctuations away from A , it is natural to look for the solution of (51) of the form

$$P(R) = Q(R) \exp\left(\frac{F(R)}{\lambda^2}\right) \quad (54)$$

where $F(R)$ is independent of λ . Plugging this into (51) and integrating over V gives a saddle point equation for $F(R)$,

$$F(R) = \max_{R_1, R_2, \dots, R_K} \left\{ -\frac{1}{2} \left(R - E + \sum_{i=1}^K \frac{1}{R_i} \right)^2 + \sum_{i=1}^K F(R_i) \right\} \quad (55)$$

The saddle point is given by the R_i that solve

$$F'(R_i) = -\frac{1}{R_i^2} \left(R - E + \sum \frac{1}{R_i} \right) \quad (56)$$

Finding the solution $F(R)$ of (55)–(56) is nontrivial. If, however, the saddle point is symmetric, $R_1 = R_2 = \dots = R_K$, the function $F(R)$ satisfies

$$F(R) = \max_{R_1} \left\{ -\frac{1}{2} \left(E - R - \frac{K}{R_1} \right)^2 + KF(R_1) \right\} \quad (57)$$

Even under this assumption, we could not find a closed expression for $F(R)$ in terms of elementary functions. One can, however, show that a solution of (57) is given by

$$F(R) = \lim_{n \rightarrow \infty} G_n(R) \quad (58)$$

where the $G_n(R)$ are defined by

$$G_n(R) = \max_{X_1, X_2, \dots, X_n} \left\{ -\frac{1}{2} \sum_{p=0}^n K^p \left(X_p - E + \frac{K}{X_{p+1}} \right)^2 \right\} \quad (59)$$

with $X_0 = R$ and $X_{n+1} = A$.

It is easy to show that (58) and (59) solve (57). First, it is clear that $G_n(R) \leq 0$ for all n and R . Second, it is easy to check that $G_n(R)$ increases with n . This can be seen by choosing the same set X_1, X_2, \dots, X_n for G_n and G_{n+1} with $X_{n+1} = X_{n+2} = A$. Since the G_n increase and are all negative, the limit (58) which defines $F(R)$ exists. That $F(R)$ satisfies (57) then follows from the observation that

$$G_{n+1}(R) = \max_{R_1} \left\{ -\frac{1}{2} \left(E - R - \frac{K}{R_1} \right)^2 + K G_n(R_1) \right\} \quad (60)$$

We tried to check the assumption that the saddle point equation (55) has a symmetric saddle point by solving this equation numerically for $K=2$ and $E=3$. The values of R_1 and R_2 which give the saddle point are shown in Fig. 4 and the numerical solution for $F(R)$ is shown in Fig. 5. We see that the saddle point is symmetric for a range of values of R around A . Outside this range, however, the saddle point is no longer symmetric and $F(R)$ seems to be constant. The rather complicated shape of $F(R)$ makes the calculation of the integrated density of states difficult, in particular because it is hard to tell if the two terms which appear in the expression (13) of $\langle \omega(E) \rangle$ are of the same order when λ is small, and because if the

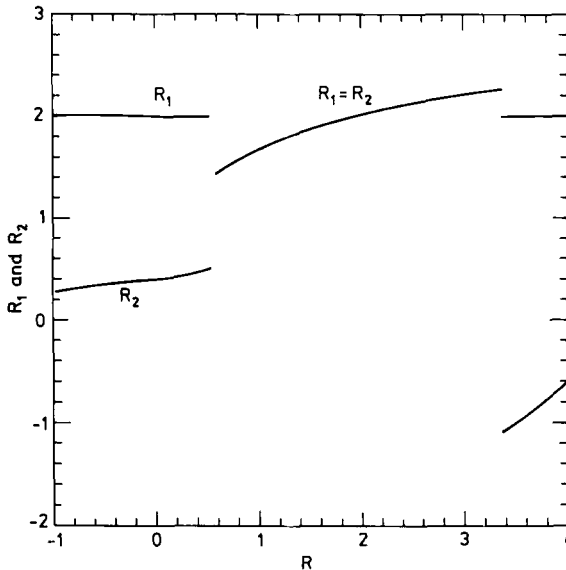


Fig. 4. The solutions $R_1(R)$ and $R_2(R)$ of the saddle point equation (55) for $K=2$ and $E=3$ as a function of R . Near the stable fixed point A , the saddle point is symmetric: $R_1(R) = R_2(R)$, while for larger and smaller values of R the symmetry is broken, $R_1(R) \neq R_2(R)$.

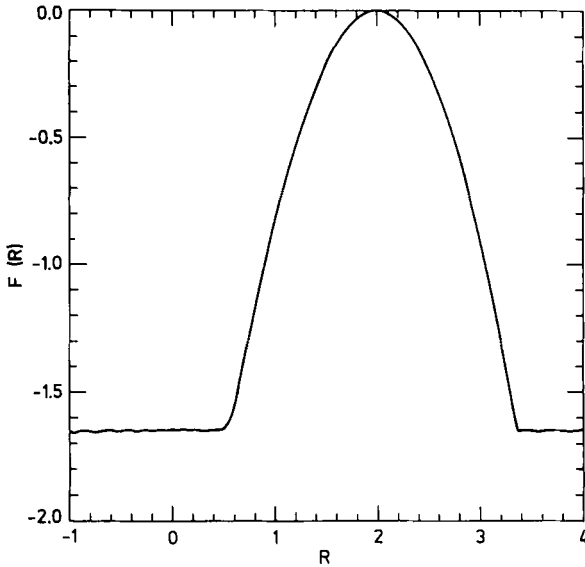


Fig. 5. Numerical solution of the saddle point equation (55) for $F(R)$ with $K=2$ and $E=3$. The function $F(R)$ seems to be constant in the range where the symmetry between $R_1(R)$ and $R_2(R)$ is broken.

terms are of the same order, the prefactor $Q(R)$ in (54) would need to be calculated. In any case, one would find a nonzero integrated density of states $\langle \omega(E) \rangle$ which would be exponentially small when $\lambda \rightarrow 0$ and which would vanish to all orders in perturbation in λ .

7. NUMERICAL ATTEMPT TO DETERMINE THE MOBILITY EDGE

Expression (49) obtained in Section 5 predicts that the mobility edge tends to the band edge value $E = 2\sqrt{K}$ as $\lambda \rightarrow 0$. This disagrees with the result of Abou-Chacra and Thouless⁽⁶⁾ that the mobility edge tends to $E = K + 1$ as λ gets small.

That the perturbative expansion might be insufficient to predict the location of the mobility edge has been discussed above: the perturbative expansion predicts that for $E > E_c$ the density of states is zero to all orders in λ , whereas one knows that the density of states never vanishes for an unbounded distribution $\rho(V)$ of potentials. We tried to show in the previous section that a way of resolving this difficulty is to have nonperturbative contributions. The same could also happen for the reflection

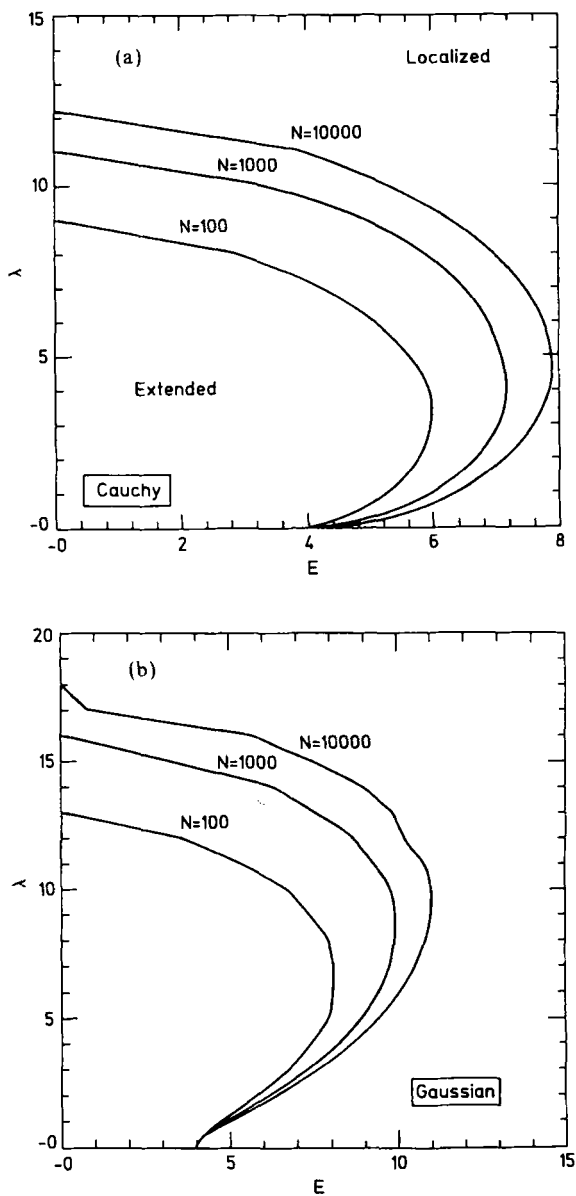


Fig. 6. (a) Monte Carlo determination as described in Section 7 of the mobility edge for Cauchy distributed disorder. Here $K = 4$. The number N of different R is 100, 1000, or 10,000. (b) Same, for the Gaussian disorder. (c) Same, for *independent* R distributed according to the Cauchy distribution (20).

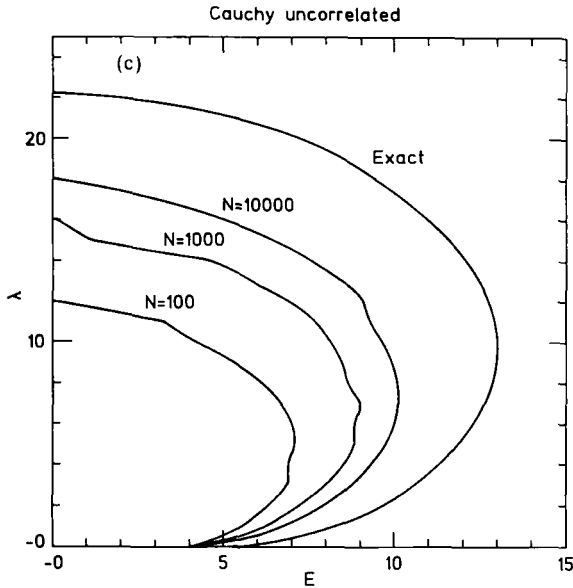


FIGURE 6 (continued)

amplitude: one could have $|r| = 1$ for $E > E_c$ to all orders in λ but with $|r| \neq 1$ because of nonperturbative effects.

One way of locating the mobility edge is to determine whether the distribution $P_{\text{real}}(R)$ is stable against imaginary perturbations. We know that if the R_i are real at the boundary, they remain real under the iteration (2). Now let us add an infinitesimal imaginary component $i\epsilon$ to the R_i at the boundary. After a finite number n of iterations of (2), the imaginary part of R_i is still infinitesimal and is proportional to ϵ . Calling this imaginary part $i\epsilon Y_i$, we have

$$Y_i = \sum_{\text{paths}} \sum_{j \in \text{path}} \frac{1}{R_j^2} \tag{61}$$

where the sum in (61) runs over all the K^n paths of n steps from site i to the boundary of the tree. If one computes the Y_i , either they go to zero as n increases, meaning that $P_{\text{real}}(R)$ is stable, or they grow with n , meaning that $P_{\text{real}}(R)$ is unstable.

7.1. Numerical Approach

We did not find an analytical way of determining whether the Y_i grow or decay under the iteration procedure. So we had recourse to a Monte

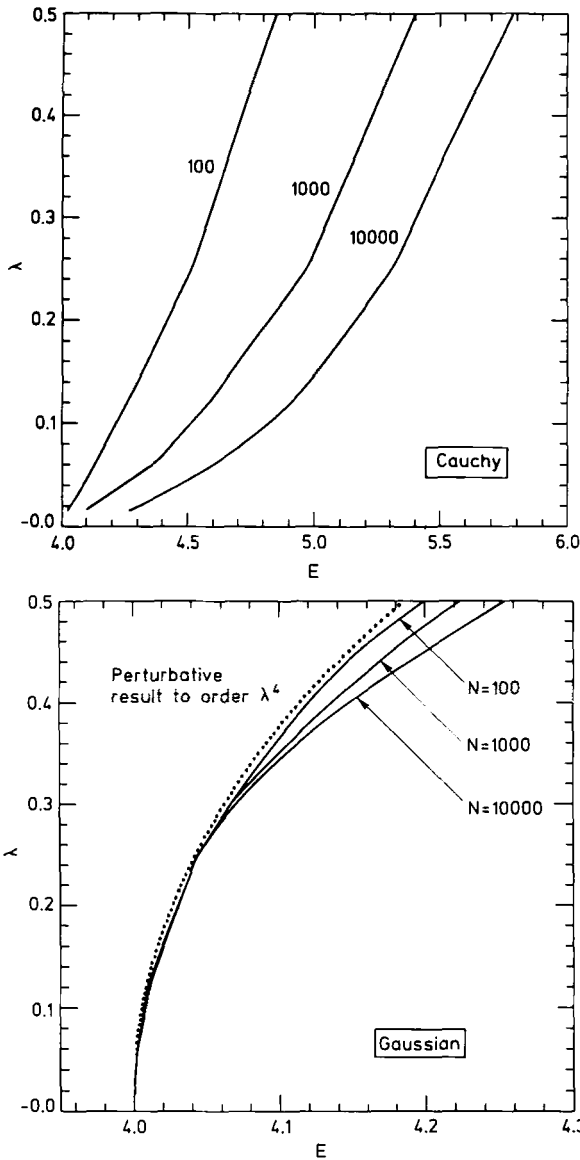


Fig. 7. Enlargements of Figs. 6a–6c showing small values of λ . Panel (b) shows a rather nice agreement with the result (49). However, as N increases, the agreement seems to become worse, indicating that the limits $N \rightarrow \infty$ and $\lambda \rightarrow 0$ do not commute. This is even more apparent for the independently distributed R , where the exact result converges in the limit $\lambda \rightarrow 0$ to $E = K + 1$ as predicted by Abou-Chacra and Thouless,⁽⁶⁾ whereas the finite- N curves converge to the band edge $2\sqrt{K}$.

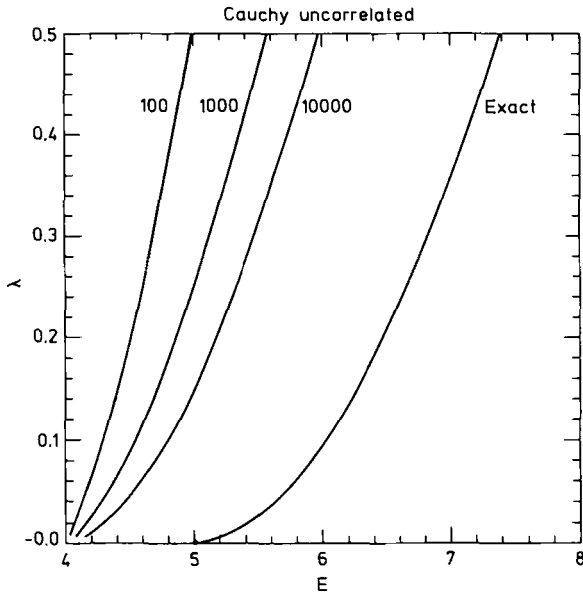


FIGURE 7 (continued)

Carlo method. We represent the distribution $P_{\text{real}}(R)$ by a sample of N points, where typically $N = 100, 1000$, or $10,000$. This means that we have N values of the R_i and N values of the Y_i . At each elementary step, we update one i chosen at random, by choosing K indices at random j_1, \dots, j_K between 1 and N and a random value of the potential V_i and we replace R_i and Y_i by

$$R_i = E - \lambda V_i - \left(\frac{1}{R_{j_1}} + \frac{1}{R_{j_2}} \cdots + \frac{1}{R_{j_K}} \right) \quad (62)$$

$$Y_i = \frac{1}{R_{j_1}^2} Y_{j_1} + \frac{1}{R_{j_2}^2} Y_{j_2} \cdots + \frac{1}{R_{j_K}^2} Y_{j_K} \quad (63)$$

We start with the Y_i of order 1 and we iterate this procedure until all the Y_i have become either very large, 10^{30} , or very small, 10^{-30} . The mobility edges estimated by this procedure are shown in Figs. 6 and 7 for the Gaussian and Cauchy distributions. The points for different values of λ are obtained for different samples, and so the roughness of the curves indicates the statistical errors.

We expect this procedure to give the true mobility edge for N infinitely large since for large N the values of $R_{j_1}, R_{j_2}, \dots, R_{j_K}$ are independent. We see

that as N increases the estimated mobility edge moves upward and to the right and so it is not so easy to predict from these data accurate values of the large- N limit. For a Gaussian potential and for small λ the results shown in Fig. 7b seem to agree well with the expression (49). Notice, however, that the agreement becomes worse as N increases. This means that even though the mobility edge in the limit $\lambda \rightarrow 0$ starts at $2\sqrt{K}$ and not $K+1$ in our simulations, we cannot conclude from the data that the mobility edge really starts at $2\sqrt{K}$ when $\lambda \rightarrow 0$, because the limits $N \rightarrow \infty$ and $\lambda \rightarrow 0$ may not commute.

7.2. The Case of Independent R

In order to test the validity of this numerical approach, it is useful to try it in an exactly soluble case. If we suppose the R_i to be independent random variables distributed according to a given probability distribution $P_{\text{real}}(R)$, one knows from the theory of direct polymers^(32,33) on a tree the exact expression of the large- n limit of $\log Y_i/n$, where the Y_i are defined by (61). To test the Monte Carlo procedure described above, we computed the ‘‘mobility edge’’ by using (63) with independent R_i chosen according to their exact probability distribution (20). Then, using the known results from the problem of directed polymers, one has for large n

$$(Y_i)_{\text{typical}} \simeq [\min_{\beta} (K \langle R^{-2\beta} \rangle)^{1/\beta}]^n \quad (64)$$

The line in the plane E, λ which separates the region of very large Y_i and very small Y_i can then be obtained exactly using the following expression for $\langle R^{-2\beta} \rangle$:

$$\begin{aligned} \langle R^{-2\beta} \rangle &= \frac{b}{\pi} \int_{-\infty}^{\infty} dR \frac{R^{-2\beta}}{(R-a)^2 + b^2} \\ &= \frac{b^{-2\beta}}{\cos(\pi\beta)} \left(\frac{b^2}{a^2 + b^2} \right)^{\beta} \cos \left[2\beta \tan^{-1} \left(\frac{a}{b} \right) \right] \end{aligned} \quad (65)$$

The exact curve for independent R_i is shown in Figs. 6c and 7c together with the results of the Monte Carlo procedure. We see that the results seem to converge rather slowly as N increases. Moreover, the limits $N \rightarrow \infty$ and $\lambda \rightarrow 0$ do not seem to commute, as the exact result tends to $K+1$ as predicted by Abou-Chacra and Thouless,⁽⁶⁾ whereas the finite- N results tend to the band edge value $2\sqrt{K}$.

In summary we see that the Monte Carlo procedure described above

can in principle be used to determine the mobility edge. However, $N=10,000$ does not seem to be large enough to resolve numerically the question of where the mobility edge starts in the $\lambda \rightarrow 0$ limit.

8. CONCLUSION

We have shown that a great deal of information on the Anderson model on a tree is contained in the random recursion (2). If we assume that under iteration of (2), the distribution of R converges to a fixed distribution $P(R)$, the problem of knowing whether the wavefunctions are extended or localized reduces to the question of the existence of a complex fixed distribution $P_{\text{complex}}(R)$. Equation (4) that $P(R)$ satisfies is in fact equivalent to those already obtained by other methods.⁽⁵⁻⁹⁾ We think, however, that our way of deriving these equations is more direct.

The main result of this work was to show that one can expand quantities of interest like the density of states, the mobility edge, or the reflection amplitude in powers of λ . This approach is not, however, entirely satisfactory because we have not fully understood the nonperturbative effects. In particular, the existence and nature of nonperturbative corrections to the complex fixed distribution $P_{\text{complex}}(R)$ remain open questions, as, by consequence, does the position of the mobility edge in the limit $\lambda \rightarrow 0$. Both our perturbative expansion and our Monte Carlo simulations indicate that the mobility edge starts at the band edge of the pure system, but nonperturbative effects could change the former prediction, and as is the case for the independent R of Section 7, the limit $N \rightarrow \infty$ and the limit $\lambda \rightarrow 0$ may not commute in the latter.

We think several important points deserve further consideration.

First, it would be nice to be able to prove mathematically that the sequence of $P_n(R)$ converges and to know under what conditions a complex fixed distribution exists. This problem is not easy because, as we discussed above, in the pure case, the sequence does not converge for energies inside the band and somehow it is the effect of a weak disorder which makes the distribution concentrate around the complex fixed point.

Second, it would be interesting to develop a nonperturbative approach, especially for the complex distribution, in order to compute at least for small λ the shape of the mobility edge. Despite our efforts, we were unable to find a method allowing us to describe $P_{\text{complex}}(R)$ for small λ in the range of energies $|E| > 2\sqrt{K}$.

One could also try to use the recursion (2) to calculate other quantities which play an important role in the localization problem, such as the inverse participation ratio.

Last, we think that the Monte Carlo procedure described in Section 7

could be used to accurately determine the position of the mobility edge by increasing N to one or ten million, though this would require a rather serious numerical effort.

APPENDIX

In this appendix we derive the relation (5) between the real and complex fixed-point distributions and the expression (14) of the integrated density of states from the expression (13). To do so, let us assume that we have a sequence of complex distributions $P^n_{\text{complex}}(r - is)$ concentrated on the lower half-plane which satisfy the recursion (3). To each of these distributions we associate a real distribution $Q^n(R)$ by

$$Q^n(R) = \frac{1}{\pi} \int_{-\infty}^{\infty} dr \int_0^{\infty} ds \frac{s}{(R-r)^2 + s^2} P^n_{\text{complex}}(r - is) \tag{A1}$$

We are going to show that the sequence of $Q^n(R)$ thus defined also satisfies (3).

From the recursion relation (3) for the complex distribution P^n_{complex} , we can rewrite (A1) as

$$Q^{n+1}(R) = \int_{-\infty}^{\infty} dr \int_0^{\infty} ds \prod_{i=1}^k \int_{-\infty}^{\infty} dr_i \int_0^{\infty} ds_i \frac{1}{\pi} \frac{s}{(R-r)^2 + s^2} \int \rho(V) dV \times P^n_{\text{complex}}(r_i - is_i) \delta\left(r - E + \lambda V + \sum_{i=1}^k \frac{r_i}{r_i^2 + s_i^2}\right) \delta\left(s - \sum_{i=1}^k \frac{s_i}{s_i^2 + r_i^2}\right) \tag{A2}$$

It is useful now to note two properties of Cauchy distributed random variables. A Cauchy distribution is a probability distribution $C(x; a, b)$ defined by

$$C(x; a, b) = \frac{1}{\pi} \frac{b}{(x - a)^2 + b^2} \tag{A3}$$

where a is real and b is real and positive. Let x_1 and x_2 be Cauchy distributed random variables with distributions $C(x_1; a_1, b_1)$ and $C(x_2; a_2, b_2)$, respectively. Then the sum $x = x_1 + x_2$ is Cauchy with distribution $C(x; a_1 + a_2, b_1 + b_2)$. Similarly, if x is distributed according to $C(x; a, b)$, the inverse $y = 1/x$ is Cauchy with distribution $C(y; a/(a^2 + b^2), b/(a^2 + b^2))$. Hence, if the real variables R_1, \dots, R_k are Cauchy distributed

with distributions $C(R_i; r_i, s_i)$, it follows for fixed V that the real variable R defined by

$$R = E - \lambda V - \sum_{i=1}^k \frac{1}{R_i} \tag{A4}$$

is distributed according to $C(R; r, s)$, where $r = E - \lambda V - \sum_{i=1}^k r_i / (r_i^2 + s_i^2)$ and $s = \sum_{i=1}^k s_i / (s_i^2 + r_i^2)$. Written out as an equation, this reads

$$\frac{1}{\pi} \frac{s}{(R-r)^2 + s^2} = \int_{-\infty}^{\infty} \prod_{i=1}^k dR_i \frac{1}{\pi} \frac{s_i}{(R_i - r_i)^2 + s_i^2} \delta \left(R - E + \lambda V - \sum_{i=1}^k \frac{1}{R_i} \right) \tag{A5}$$

If we substitute (A5) into (A2) and use (A1), namely that

$$Q^n(R) = \int_{-\infty}^{\infty} dr_i \int_0^{\infty} ds_i \frac{1}{\pi} \frac{s_i}{(R - r_i)^2 + s_i^2} P_{\text{complex}}^n(r_i - is_i) \tag{A6}$$

it follows that the $Q_n(R)$ also obey (3). Assuming that in the limit $n \rightarrow \infty$ the $Q^n(R)$ converge establishes (5).

Let us now see how (14) can be obtained from (13). Expression (13) can be rewritten as

$$\begin{aligned} \langle \omega(E) \rangle = & -\frac{1}{\pi} \text{Im} \left\{ \frac{K-1}{2} \int_{-\infty}^{\infty} P_{\text{real}}(R) dR \right. \\ & \times \int_{-\infty}^{\infty} P_{\text{real}}(R') dR' \log \left(R' - i\varepsilon - \frac{1}{R - i\varepsilon} \right) \\ & \left. + \frac{K+1}{2} \int_{-\infty}^{\infty} P_{\text{real}}(R) dR \log(R - i\varepsilon) \right\} \tag{A7} \end{aligned}$$

where $-i\varepsilon$ is an infinitesimal imaginary part. One can then replace $P_{\text{real}}(R)$ in this expression by (5). Using the residue theorem to do the integral over the real variable R gives (14).

ACKNOWLEDGMENTS

We thank M. Aizenman and S. Ruffo for useful discussions.

REFERENCES

1. P. W. Anderson, *Phys. Rev.* **109**:1492 (1958).
2. D. J. Thouless, *Phys. Rep.* **13**:93 (1973).
3. B. Souillard, in *Chance and Matter* (Les Houches XLVI, 1986), J. Souletie, J. Vannimenus and R. Stora, eds. (1987).

4. B. Bulka, B. Kramer, and A. MacZinnon, *Z. Phys. B* **60**:13 (1985).
5. R. Abou-Chacra, P. W. Anderson, and D. J. Thouless, *J. Phys. C* **6**:1734 (1973).
6. R. Abou-Chacra and D. J. Thouless, *J. Phys. C* **7**:65 (1974).
7. H. Kunz and B. Souillard, *J. Phys. Lett. (Paris)* **44**:L411 (1983).
8. A. D. Mirlin and Y. V. Fyodorov, *Nucl. Phys. B* **366**:507 (1991).
9. A. D. Mirlin and Y. V. Fyodorov, *J. Phys. A* **24**:2273 (1991).
10. Y. Kim and A. B. Harris, *Phys. Rev. B* **31**:7393 (1985).
11. V. Acosta and A. Klein, *J. Stat. Phys.* **69**:277 (1992).
12. T. Kawarabayashi and M. Suzuki, *J. Phys. A* **26**:5729 (1993).
13. K. B. Efetov, *Sov. Phys. JETP* **61**:606 (1985).
14. B. Shapiro, *Phys. Rev. Lett.* **50**:747 (1983).
15. J. T. Chalker and S. Siak, *J. Phys. Cond. Matt.* **2**:2671 (1990).
16. B. Derrida and G. J. Rodgers, *J. Phys. A* **26**:L457 (1990).
17. B. Derrida and E. Gardner, *Phys. (Paris)* **45**:1283 (1984).
18. F. Wegner, *Z. Phys. B* **44**:9 (1981).
19. T. Spencer, in *Critical Phenomena, Random Systems, Gauge Theories* (Les Houches XLIII, 1984), K. Osterwalder and R. Stora, eds. (1986).
20. L. Pastur and A. Figotin, *Spectral Properties of Disordered Systems in the One-Body Approximation* (Springer-Verlag, 1991).
21. G. J. Rodgers and A. J. Bray, *Phys. Rev. B* **37**:3557 (1988).
22. G. J. Rodgers and C. De Dominicis, *J. Phys. A* **23**:1567 (1990).
23. Y. V. Fyodorov, A. D. Mirlin, and H. J. Sommers, *J. Phys. I (Paris)* **2**:1571 (1992).
24. D. Dhar and R. Ramaswamy, *Phys. Rev. Lett.* **54**:1346 (1985).
25. M. Aizenman and S. Molchanov, *Commun. Math. Phys.* **157**:245 (1993).
26. M. Aizenman, preprint (1993).
27. J. M. Luck, Systèmes désordonnés unidimensionnels, Aléa, Saclay (1992).
28. M. Kappus and F. Wegner, *Z. Phys. B* **45**:15 (1981).
29. C. J. Lambert, *Phys. Rev. B* **29**:1091 (1984).
30. A. Bovier and A. Klein, *J. Stat. Phys.* **51**:501 (1988).
31. M. Campanino and A. Klein, *Commun. Math. Phys.* **130**:441 (1990).
32. E. Buffet, A. Patrick, and J. V. Pule, *J. Phys. A* **26**:1823 (1993).
33. B. Derrida, M. R. Evans, and E. R. Speer, *Commun. Math. Phys.* **156**:221 (1993).